

THE TRANSVERSE MAGNETORESISTANCE OF  
HIGH STRENGTH COPPER ALLOYS

by

Richard A.E. Bolton

A thesis submitted to the Faculty of  
Graduate Studies and Research in partial  
fulfilment of the requirements for the  
degree of Master of Science.

Department of Physics,  
McGill University,  
Montreal.

February 1963

Richard Bolton

THE TRANSVERSE MAGNETORESISTANCE OF HIGH STRENGTH  
COPPER ALLOYS

ABSTRACT

Two high strength alloys of copper, .12% Zr and .3% Cr, were investigated for residual resistance and transverse magnetoresistance at fields up to  $10 \frac{\text{Vs}}{\text{m}^2}$ . The measurements were made at liquid nitrogen and liquid helium temperatures.

The material was in the form of wire of diameter .0025 inch. For comparison purposes commercial grade copper magnet wire, #40 gauge, was also tested.

The copper showed a relative increase in resistivity  $\frac{\Delta\rho}{\rho}$  of 2.5 at  $10 \frac{\text{Vs}}{\text{m}^2}$ . Corresponding figures for the zirconium and chromium alloys were up to 1.0 and up to .065 respectively.

This wide variation in magnetoresistance is shown to be mainly due to the difference in residual resistance, by Kohler's Rule. The maximum resistance ratios  $\frac{R_{\text{max}}}{R_{\text{res}}}$  obtained were 100 for copper, 70 for Zr-Cu, and 30 for Cr-Cu.

When the results are plotted on Kohler diagrams, the zirconium alloy shows transverse magnetoresistance from 25% to 80% higher than copper. The chromium alloy varied from 20% less to 30% higher than copper.

## ACKNOWLEDGEMENTS

The writer would like to express his indebtedness to Dr. D.R. Stevenson for suggesting the problem and supervising the research. He would also like to thank the National Magnet Laboratory of the Massachusetts Institute of Technology for the use of their high field magnet installation, and Dr. S.C. Collins of the same Institution for preparation facilities.

The work was supported in part by the United States Navy, Office of Naval Research, and by the Defence Research Board. The writer is grateful to the National Research Council for the Studentship held in 1962-63.

## CONTENTS

1. Introduction	1
2. Experimental Apparatus and Procedure	
(a) Preparation of Samples	7
(b) Low Temperature Apparatus	11
(c) Magnet	16
(d) Measuring Technique	17
3. Results and Discussion	20
Appendix	
A. Transverse Magnetoresistance of Two Band Model	31
B. Ice Point Resistivity of Annealed Samples	33
References	34

## 1. INTRODUCTION

Consideration of either plane waves or Bloch functions shows that a perfect lattice introduces no attenuation to these waves. The difference between the transmission of waves with free electron theory and in a periodic structure is the appearance of discontinuities in the relation between energy and wave vector.<sup>1</sup> This gives rise to the concepts of energy bands and Brillouin Zones.<sup>2, 3.</sup>

The band structure of a solid will determine its electrical properties.<sup>1</sup> If a substance has its uppermost occupied band completely filled at the absolute zero of temperature, and if the energy gap to the next band is large compared to  $kT$ , the Fermi-Dirac distribution will not permit population of this next band to any significant extent, and the solid will be an insulator. A filled band, being symmetrical has only pairs of states with wave vectors ( $\vec{k}$ ) which will balance out. Conduction is caused by a shift from the equilibrium distribution to one in which a particular direction of  $\vec{k}$  is favoured. If all states are occupied, no shift is possible.

A solid will have the highest electrical conductivity when the uppermost band is only half occupied. This situation provides the maximum number of electrons in states which will not counteract each other. Thus the alkali and noble metals show high conductivity since the s-band contains one electron where two could exist by Pauli's Principle.

However once a suitable number of carriers has been established, the conductivity should be infinite. Resistance must be attributed to

deviations from true periodicity of the lattice. In general this lack of periodicity can be separated into two classes: physical and thermal.

Under physical imperfections are considered impurity atoms in the lattice sites and imperfections in construction of the lattice itself. Typical of the latter category are vacancies at lattice sites, extra atoms between sites, called interstitials, and dislocations in the crystal such as grain boundaries and stacking faults.<sup>4</sup>

The thermal imperfection of the lattice is due to vibration of the atoms about their lattice sites. Since the atoms are coupled, they vibrate dependently with the frequencies of the normal modes of the crystal.<sup>5</sup> These vibrations contain the internal energy of the lattice, and as the internal energy decreases with temperature, so does the resultant resistance. The resistivity at the absolute zero of temperature is called the residual resistivity, and is due to physical imperfections alone.

Matthiessen's Rule states that the physical and thermal effects do not overlap - that is, the resistivity due to **physical** imperfection is independent of the temperature. This rule, which usually holds<sup>6</sup> for small concentrations of impurity, was formulated by Matthiessen in 1857. It can be stated as follows:

$$\rho = \rho_T + \rho_i$$

$\rho$  = total resistivity  
 $\rho_T$  = resistivity due to thermal motion  
 $\rho_i$  = resistivity due to physical imperfection

If the concentration of impurities is small, one would expect the

same resistance from thermal motion as for the pure host metal. In Gruneisen's relation<sup>6,7</sup> for the resistivity as a function of temperature, the elastic properties of the lattice enter only through the Debye characteristic temperature, which, being a scalar representing the average of the directional properties of the lattice structure, would not be expected to vary significantly with small alterations to the lattice.<sup>6</sup> In practice it is found that the best fit of experiment to theory requires slightly different values of the characteristic temperature from those obtained from specific heat experiments.<sup>6</sup>

When a magnetic field is applied to a conductor with a current flowing in it, either the current is deflected, or a transverse electric field is set up, depending on the boundary conditions, the magnetic field being perpendicular to the current. This is the Hall Effect, and now in general the current and electric field are no longer parallel and we write<sup>8</sup>

$$E_i = \rho_{ik} j_k \quad (\text{repeated index summed})$$

where the  $E_i$  are the Cartesian components of the electric field,  $j_k$  the components of the current density, and  $\rho$  is the resistivity tensor. We assume there are no thermal gradients to eliminate Thompson and related effects.

If we assume the conductor to be isotropic, the tensor  $\rho$  must be invariant with respect to arbitrary rotation about the magnetic field  $\vec{B}$ . If  $\vec{B}$  is along the z axis the tensor must take the form

$$\begin{pmatrix} \rho_{\perp} & \rho_H & 0 \\ \rho_H & \rho_{\perp} & 0 \\ 0 & 0 & \rho_{\parallel} \end{pmatrix}$$

where  $\rho_{\perp}$  is the resistivity perpendicular to B,  $\rho_{\parallel}$  is that parallel to B, and  $\rho_H$  is the Hall resistivity.

If  $\rho_{\perp}$  and  $\rho_{\parallel}$  are not dependent upon B, then the resistivity in the direction of the current is not a function of B, for it is<sup>9</sup>

$$\rho_{ij} l_i l_j = \rho_{\parallel} \cos^2 \theta + \rho_{\perp} \sin^2 \theta$$

where the  $l_i$  are the direction cosines of the current direction and  $\theta$  is the angle between the current and the magnetic field. Thus for the single band model we are considering, the appearance of a Hall voltage does not change the resistivity in the direction of the current, and this is what is measured in any experiment on a length of rod or wire.<sup>8</sup>

A two band model (Appendix A) will show a transverse magnetoresistance but no longitudinal effect, merely as a consequence of the appearance of Hall voltages. The two bands must have different Hall resistivities. This model is not adequate to explain the experimental results for metals, since they exhibit a longitudinal effect less than but of the same order of magnitude as the transverse effect.<sup>5</sup>

Application of Onsager's Relations to the resistivity tensor shows that<sup>8,9,10.</sup>

$$\rho_{ki}(B) = \rho_{ik}(-B)$$

that is

$$\begin{aligned} \rho_{\perp}(B) &= \rho_{\perp}(-B) \\ \rho_{\parallel}(B) &= \rho_{\parallel}(-B) \\ \rho_H(B) &= -\rho_H(-B) \end{aligned}$$



in the isotropic case we are considering. Thus  $\rho_{\perp}$  and  $\rho_{\parallel}$  are even functions of B while  $\rho_{H}$  is an odd function. Thus, for small enough fields, the change in  $\rho_{\perp}$  and  $\rho_{\parallel}$  should vary as  $B^2$ .

Mott and Jones show an expression varying as  $B^2$  valid for small fields at temperatures above the Debye Characteristic temperature.<sup>11,12</sup> Both these conditions are violated in the present experiment.

Lifshitz, Azbel and Kaganov<sup>13</sup> produced a theory which predicts either a quadratic field dependence or a saturation at high fields.<sup>10</sup> However, Kapitza, and more recently Chambers, found a linear field dependence at high fields.<sup>15,16</sup> Ziman shows how the theory will predict a linear increase when averaged over all directions for a polycrystalline sample.<sup>10,14</sup> He makes no attempt to justify his averaging procedure except to say that the results fit experiment remarkably well.

Titeica's theory of quantized electron orbits for high fields predicts a linear increase above a critical field.<sup>17</sup> Unfortunately, this critical field occurs at about  $10^4 \frac{Vs}{m}$ , which is too high to account for experimental results.

It is found that magnetoresistance follows the rule

$$\frac{\rho(B, T) - \rho(0, T)}{\rho(0, T)} = \frac{\Delta \rho}{\rho} = F\left(\frac{B}{\rho(0, T)}\right)$$

where T is the absolute temperature. F(X) is a function which is independent of temperature. The effect of temperature enters only in the argument in  $\rho(0, T)$ . This rule is due to Kohler<sup>18</sup> and can be justified from the Boltzmann Transport Equations on the assumption

that there exists a relaxation time.<sup>10</sup>

To illustrate the rule  $\frac{\Delta \rho}{\rho}$  can be plotted against  $\frac{B}{\rho(0, \tau)}$ . It is more convenient, however, to plot against  $\frac{\rho(0, 273^\circ K)}{\rho(0, \tau)} B$ , as this avoids absolute measurements.<sup>8,10</sup> If the ice point resistivities of different samples are the same, plotting in this way (Kohler diagram) will provide comparisons of magneto resistance which are independent of the residual resistance of the samples.

## 2. EXPERIMENTAL APPARATUS AND PROCEDURE

### (a) Preparation of Samples

Since mechanical strain and working of the metal increase the number of imperfections in the lattice and thereby increase the residual resistance, the wires were purchased uninsulated. This permitted controlled handling and also allowed for further heat treatment. The diameter of the chromium (.3% Cr.) and zirconium (.12% Zr.) alloy wires was .0025 inch.

As it was required that five samples fit in the tailpiece of the cryostat, and as the helium compartment of the tailpiece was only 3/4" in diameter, it was decided to wind the wire on cylindrical fibre formers one-eighth inch in diameter and one inch long (Fig. 1). The samples were to have a room temperature resistance of about fifty ohms.

Initially the wires were insulated by suspending twenty foot lengths horizontally and painting them with Glyptal Paint, using a soft artist's brush. The wire was then wound on the formers with a coat of Glyptal between layers, and each layer was allowed to dry for twenty four hours before the application of the next layer. Even so, some considerable difficulty was encountered when the dried Glyptal dissolved in that being applied, causing shorts between layers.

The samples constructed in this manner showed high residual resistance. In order to investigate this further, lengths of the wire were wound on two inch lengths of half inch polystyrene cylindrical rod. A fine thread was cut in the outside of these formers to permit

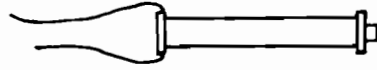


Figure 1. Fibre Former

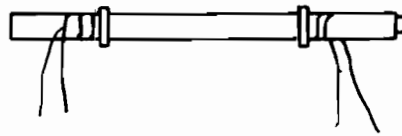


Figure 2. Micarta Former

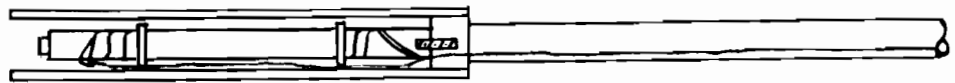


Figure 3 . Micarta Former on Rod

winding without insulation. Current and voltage leads were soldered to the samples and the formers were attached to the end of a thin four foot length of cupro-nickel tubing. Using this rod the samples were immersed in liquid nitrogen and liquid helium in the laboratory dewars. At each temperature the resistances of the samples were taken and the resistance ratios calculated. The results confirmed the previous ones, and therefore an attempt was made to improve the resistance ratio by heat treatment.

For annealing the wire was wound on threaded brass forms cut from one inch tubing. The best results were obtained from annealing for twelve hours at 500° C in an atmosphere of argon, followed by quenching in distilled water. A few samples survived 600° for the same length of time, but for the most part they were too brittle to wind.

The maximum resistance ratios  $\frac{R_{300^{\circ}K}}{R_{4.2^{\circ}K}}$  obtained were 70 for the zirconium alloy, and 30 for chromium. The resistance ratio of the pure copper magnet wire as purchased was 100.

The Glyptal paint would not wet the wire after annealing because of a layer of oxide on the surface, and another method of winding was devised. Two wires were wound simultaneously side by side, and then one of them was unwound leaving a uniform spacing between each turn. Glyptal cement thinned with acetone was painted on before the unwinding of the dummy wire to keep the sample wire in place. Finally the sample was given a coat of Glyptal paint for protection. Because of continued trouble with interlayer shorts the samples were limited to one layer. New formers were constructed from micarta such that

the leads could come from both ends instead of just one (Fig. 2).

The original samples had but two leads, the current and voltage leads being attached at the terminal board below the samples in the cryostat. It was decided to attach insulated leads (#40 gauge) directly to the sample, and to keep the potential lead inside the current junction. The main advantage of this change was that all loose wire was properly covered with tough insulation. This eliminated the possibility of accidental shorts in the crowded end section of the cryostat tailpiece where the twenty leads were connected to the lead-in wires.

None of the samples constructed in this manner showed as high resistance ratios as had been obtained previously. This was probably due to the cold work introduced by the winding on the smaller diameter former, as this occurred as well with the pure copper, wound directly from the supply spool.

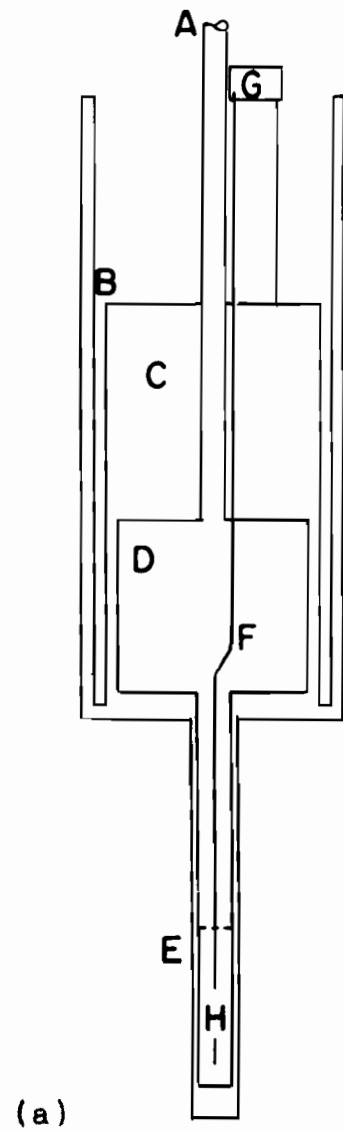
(b) Low Temperature Apparatus

Two cryostats were constructed for the low temperature measurements. The first had five samples permanently installed, and the second was designed for insertion of one sample coil at a time without disassembly. Both cryostats were constructed mainly of brass with stainless steel filling tubes and a stainless steel section to isolate the liquid nitrogen section of the double dewar from room temperature.

The first cryostat (Fig. 4a) had a lead-in tube from a junction box on top down to the sample area in the tailpiece. The junction box was brass with a bakelite top, and the external leads were slipped through holes in the bakelite, knotted, and glued in place. The short ends protruding from the knots were trimmed and the internal leads (#40 Nyclad copper) were soldered to them.

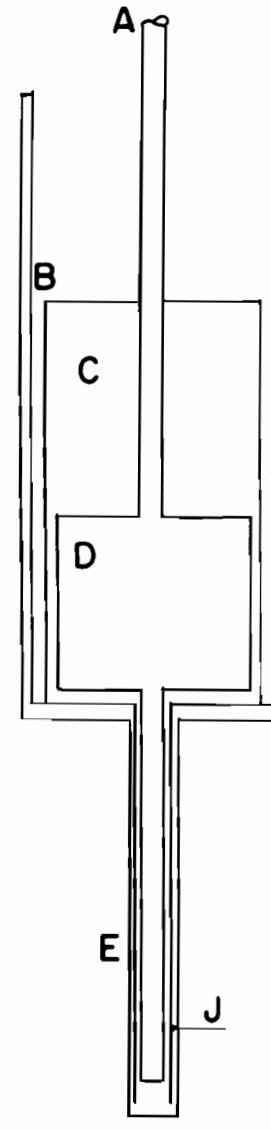
The five sample coils were mounted vertically in the tailpiece so that the longitudinal magnetic field in the solenoid would be perpendicular to the current, and the transverse magnetoresistance would be measured.

The formers were held at the top by a brass plug (Fig. 5a) which had five holes to seat the samples, five holes for the passage of liquid helium, and one central hole for the lead-in tube. Mounted in this way, the samples were completely immersed in the coolant. The brass lead-in tube was soldered to the plug and extended down the axis in the middle of the ring of samples. The bottom ends of the samples were held by a disk of teflon with seats cut in it. A



(a)

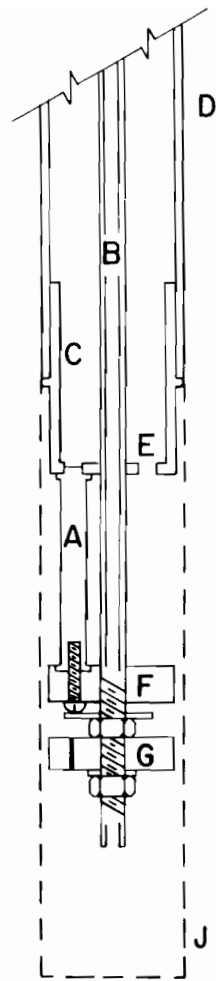
- A - Filling Tube
- B - Liq. Nitrogen Area
- C - Vacuum Space
- D - Helium Pot
- E - Tailpiece
- F - Lead-in Tube
- G - Junction Box
- H - Sample Area
- J - Thermal Shield



(b)

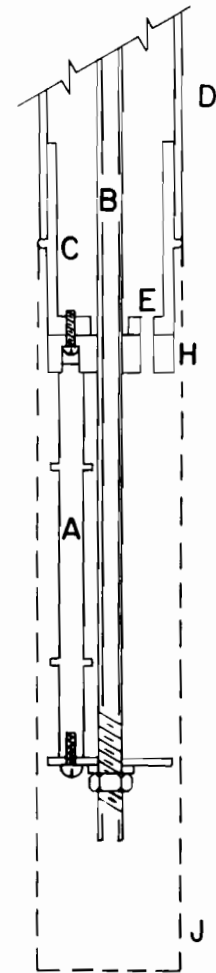
Figure 4. Cryostats





(a)

- A - Sample Former
- B - Lead-in Tube
- C - Brass Plug
- D - Helium Tube
- E - Helium Hole
- F - Teflon Seat
- G - Bakelite Terminal Board
- H - Bakelite Seat
- J - End Cap



(b)

Fig. 5. Sample Mounting

brass screw was put through the teflon into each former. The teflon disk was held in place by a brass washer and a nut threaded on the tube. Below this was a piece of thick bakelite with drilled copper inserts to act as a terminal board. The lead wires were soldered to the sample leads and then the joints were soldered into the holes in the inserts. The lead-in wires were protected by a polyethylene tube inside the brass tube.

Unfortunately there was a heat conduction path from the brass plug down the lead-in tube, through the nut and washer and up the screws into the formers. This caused the formers to swell when the end cap was soldered on, breaking the samples.

For this reason the mounting of the samples was modified as follows (Fig. 5b). New formers were made from micarta (Fig. 2) with half inch blank ends. A piece of thick bakelite was placed between the brass plug and the samples, and the central hole in the plug was reamed to clear the lead-in tube. The bakelite was held by small brass screws. The seats for the top ends of the formers were cut in the bakelite as were holes for the passage of the liquid helium. The bottoms of the samples were held with a thin bakelite plate, washer and nut, with screws through the bakelite into each former. The leads from each sample were cut fairly short and soldered to the lead-in wires. Then the joints were cemented to the blank ends of the formers. A sheet of thin teflon was wrapped around the assembly, and the cap was soldered on.

A second cryostat (Fig. 4b) was constructed as insurance against failure. The outer dimensions were similar to those of the first one, but the method of introducing samples was different. This cryostat had a thinner helium tube in the tailpiece to allow a brass tubular shield to be between it and the outer tube. This shield was soldered to the bottom of the nitrogen bath and in effect extended the nitrogen shielding down the tailpiece.

The sample formers were connected to a small brass plug in the end of a long thin tube, and brass tubular shields were placed around them for protection (Fig. 3). The sample leads were brought up the outside of the tube and soldered to external leads at the top. These sample holders were inserted in turn down the filling tube of the second cryostat, after the coolant had been transferred.

(c) Magnet

The high field magnet used in the experiment was a Bitter Solenoid belonging to the National Magnet Laboratory of Massachusetts Institute of Technology. The solenoid had an inner bore of 1.125 inch and could produce a maximum field of about  $10 \frac{\text{Vs}}{\text{m}^2}$  ( $10^5$  gauss).

The fields were intended to be available for any length of time, but owing to the warm temperature of the external cooling water to the heat exchanger, and to an increase in the internal resistance of the magnet itself, the duration of the maximum fields was limited. The cooling water was supplied to the magnet by two three inch hoses at a pressure of about 100 p. s. i. .

The current supply was a regulated system capable of producing ten thousand amperes. Calibration data for the magnet show that ten thousand amperes represents  $10.4 \frac{\text{Vs}}{\text{m}^2}$  and that the relation is very nearly linear. We shall assume that one thousand amperes is equivalent to  $1 \frac{\text{Vs}}{\text{m}^2}$  .

(d) Measuring Technique

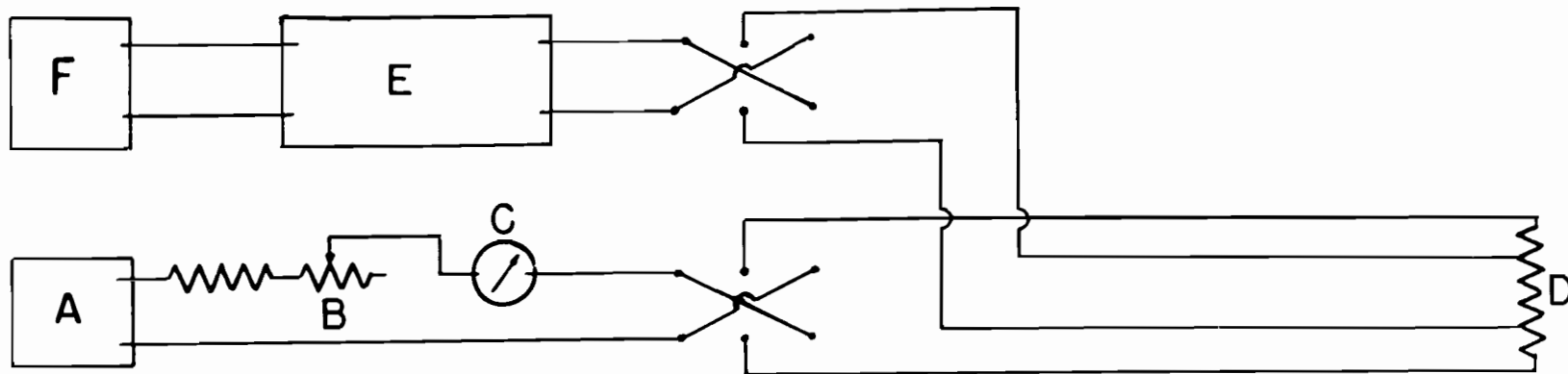
The resistance was determined by measuring with a potentiometer the voltage produced by the passage of a fixed current. This current was provided by a General Radio Regulated Power supply fed through a large resistor and helipot to provide a constant current source (Fig. 6).

The voltage was measured with a Leeds and Northrup K-2 Potentiometer, using a Keithley 150 Microvolt-ammeter as a balance detector instead of the more usual galvanometer. The response time of this arrangement was very short, and measurements could be made rapidly.

Reversing switches were installed in the current and voltage leads to allow easy measurement of the resistance in both directions. The first cryostat had one common current lead for all five samples, and the other three leads of the appropriate sample were selected by means of a switch box.

Some trouble was experienced with ground loops, but this was eliminated by floating the power supply.

The measuring current was 10 ma. Readings of resistance in both directions were taken at liquid nitrogen ( $77^{\circ}$  K) and liquid helium ( $4.2^{\circ}$  K) temperatures at intervals of one thousand amperes ( $1 \frac{V}{m^2}$ ) up to the maximum. Only zero field readings were taken at room temperature as the samples tended to heat up when the magnet was on, owing to the increase in temperature of the magnet itself.



- A - Regulated Power Supply
- B - Current Control
- C - Milliammeter
- D - Sample
- E - Potentiometer
- F - Microvolt - Ammeter

Figure 6. Measuring Circuit

The anticipated added convenience of having the samples permanently installed in the cryostat, and of being able to select the one under test by a switch was not realized. This was because the magnet could barely be left on at the maximum fields for long enough to measure the resistance of the five samples without overheating. For this reason it was necessary to alternate high and low fields to allow the magnet to cool down.

With the second cryostat, a sample was inserted and the field was started at maximum and brought down in steps to zero. In this way any hysteresis effects that might have been present were avoided. That is, only the descending portion of the curve would be plotted, not a mixture of points from both sections.

The resistance of the samples at the ice point was also measured in order to provide a fixed reference point.

### 3. RESULTS AND DISCUSSION

When the magnetic field was off, the values of the resistance in opposite directions agreed very closely, usually to within one unit in the fourth significant figure. However, with the field on, there was usually a marked discrepancy. The difference varied from sample to sample and from reading to reading for any one sample. The order of magnitude was fairly constant and this difference represented a stray voltage of about  $1.3 \times 10^{-4}$  volt on the average. The average for any one sample varied from  $.8 \times 10^{-4}$  to  $2.0 \times 10^{-4}$  volt. In further discussion the average of the resistance in the two directions is used. Since the discrepancy represents a constant voltage, the effect is less at higher fields where the resistance and hence the voltage being measured are higher.

With the second cryostat it was noticed that the zero field resistances of the samples were different after they had been subjected to the field. In all cases but two, the resistance was less afterwards and in one case there was no change. The average size of the change is about .05% of the initial resistance. The final value is used for calculation since it represents the point on the downward curve if hysteresis effects are present. In general the points taken from the second cryostat lie closer to a smooth curve than do those from the samples permanently mounted. This probably is because in the former case the readings were taken in regular descending order, whereas the others were alternated between high and low fields.



As a check on the validity of Matthiessen's Rule, and on the invariance of the temperature dependent component of resistance with addition of impurity, the zero field data was reduced as follows. The resistance of each sample at  $4.2^{\circ}$  K was subtracted from that at  $77^{\circ}$  K and  $273^{\circ}$  K. The resistance at  $4.2^{\circ}$  K represents the residual resistance on the assumption that at this temperature the thermal component is negligible. Thus the ratio of these two reduced resistances should be the ratio of the thermal components at  $77^{\circ}$  K and  $273^{\circ}$  K. This ratio should be the same for all samples, if the law of temperature variation is the same, and if Matthiessen's Rule is valid (Table 1, Column 3).

The mean value found for this ratio is  $.134 \pm .0117$ . This R.M.S. deviation from the mean is equivalent to  $\pm 8.7\%$ . Tabled values of the Grüneisen Function,<sup>6</sup> using  $\Theta = 333^{\circ}$  K for the characteristic temperature of copper, give the value of this ratio as .125. This differs from the experimental mean value by 7.4%, which is within the R.M.S. deviation. Supporting the assumption that  $R_{4.2^{\circ}K}$  is essentially the residual resistance, the tables give the ratio of thermal components at  $4.2^{\circ}$  K to that at  $273^{\circ}$  K the value  $6 \times 10^{-7}$ .

Inspection of the resistance ratios  $\frac{R_{273^{\circ}K}}{R_{4.2^{\circ}K}}$  obtained (Table 1, Column 4) shows that the zirconium alloy performed better in this respect than did the chromium. The chromium concentration is .3% compared to .12% for the zirconium. These concentrations represent atomic percentages of .37% and .084% respectively. All samples had received identical heat treatment of twelve hours at  $500^{\circ}$  C. As

mentioned previously these ratios compare unfavourably with those obtained with larger diameter formers.

When comparing the data obtained in the magnetic field and plotted on Kohler diagrams, it is assumed that all samples have the same ice point resistivity (Appendix B). Experiments to determine the actual resistivity were not feasible, and this assumption allows direct comparison.

The behaviour of typical samples is indicated in Figure 7 and Figure 8. On these graphs, the overlap sections of the measurements at  $4.2^{\circ}$  K and  $77^{\circ}$  K are plotted to illustrate Kohler's Rule. All points should lie on the same curve. Agreement is to within about 15%. With pure copper the agreement is not as good, but the conditions are more severe since the resistance ratio is higher.

Figure 9 contains all the Kohler plots for the zirconium alloy with pure copper as a reference, all at liquid helium temperature. Figure 10 contains the graphs of the three chromium alloy samples at  $4.2^{\circ}$  K. The points for copper are outside the range of this graph.

When all the results taken at liquid helium temperature are plotted on a logarithmic Kohler diagram (Figure 11), several significant details obtain. The curves are all very nearly straight, the slope being about 1.5, and are concave downwards. This suggests that the magnetoresistance is changing from the square law predicted for low fields to the linear relation found by Kapitza and by Chambers. In spite of the large variation in  $\frac{\Delta\rho}{\rho}$  from .06 for Cr-Cu to 2.5 for

copper, both at maximum field, the graphs lie very close together on the Kohler diagram. This shows that the large differences in  $\frac{\Delta \rho}{\rho}$  are due more to difference in the residual resistance than to differences in the magnetoresistance function of  $\frac{B}{\rho(0i)}$ .

The chromium alloy plots lie in the lower section of Figure 11 since they show low resistance ratios. Two of the three show less magnetoresistance than the copper; that is, their plots lie below the extrapolation of the graph of copper. The third sample shows a higher effect. The graphs for zirconium copper all lie above copper in Figure 11. Two are coincident, a third lies close to them and the fourth is considerably higher.

Rough estimates can be made of the vertical separation of each curve from the curve for copper. These are shown in Table 1, Column 5. The estimates for chromium copper are based on extensive extrapolation and hence are very crude. The zirconium alloy samples varied from +80% to +25%, the chromium from +30% to -20%.

The curves for zirconium copper, and to a lesser extent the chromium alloy, show more curvature than does the pure copper. Thus at the high end the curves are closer to those of copper.

The relative increase in resistance,  $\frac{\Delta \rho}{\rho}$  of 2.5 for copper at  $10 \frac{Vs}{m^2}$  agrees closely with the results of Olsen.<sup>19</sup>

The absolute accuracy of any one measurement depends on the uncertainty of the potentiometer reading, the accuracy of the initial current setting, and the regulation of the current supply.

The initial current setting was probably only accurate to 1%; however, since we are measuring ratios of resistance, this does not affect the results. The current was constant to one part in  $10^4$  as checked by measurements over a period of an hour on a standard resistor.

The potentiometer readings were to five significant figures, and the results were calculated from

$$\frac{\Delta\rho}{\rho} = \frac{R_B - R_0}{R_0} = \frac{R_B}{R_0} - 1 = \frac{V_B I_0}{V_0 I_B} - 1$$

where  $R_B$ ,  $V_B$ ,  $I_B$  are resistance, voltage and current at field B, and  $R_0$ ,  $V_0$ ,  $I_0$  refer to condition  $B=0$ . The final accuracy will depend markedly on the proximity of the value of  $R_B$  to  $R_0$ . When the resistance ratio is high, and as a consequence of Kohler's rule so is the magnetoresistance, the accuracy will be good, especially at high fields.

Another factor, which affects the accuracy of the calculated results, is the difference in the resistance taken in opposite directions. The discrepancy, since it appears to be caused by a stray potential of relatively constant magnitude, is larger when the potentiometer is used on the sensitive range. The graphs are smooth to within the order of magnitude of the difference, and therefore it is assumed that taking the average of the two readings eliminates the effect. Nevertheless, this is probably the limiting factor in the accuracy, and the cause of scatter of points from a smooth curve when this occurs at high fields and high resistance ratios, where the aforementioned accuracy is good.

EXAMPLES OF POSSIBLE ERROREx (a) Good Conditions

$$\text{Sample A, copper, } 4.2^{\circ} \text{ K} \quad B = 10 \frac{\text{Vs}}{\text{m}^2}$$

$$V_o = (11428 \pm 1) \times 10^{-7} \text{ volt} = 11428 \times 10^{-7} \text{ volt} \pm .00875\%$$

$$V_B = \left\{ \begin{array}{l} 39213 \pm 1 \\ 40618 \pm 1 \end{array} \right\} \times 10^{-7} \text{ volt} \quad \text{avg } V_B = \begin{array}{l} (39916 \pm 2) \times 10^{-7} \text{ volt} \\ = 39916 \times 10^{-7} \text{ volt} \pm .00502\% \end{array}$$

$$\frac{I_o}{I_B} = 1.0000 \pm .01\%$$

$$\begin{aligned} \frac{R_B}{R_o} &= 3.4928 \pm .0238\% \\ &= 3.4928 \pm .000682 \end{aligned}$$

$$\frac{\Delta \rho}{\rho} = \frac{R_B}{R_o} - 1 = 2.4928 \pm .000682$$

$$\frac{\Delta \rho}{\rho} = 2.4928 \pm .0274 \%$$

This is accuracy to within one part in the fourth figure.

Ex (b) Poor Conditions

$$\text{Sample D, Cr-Cu - } 4.2^{\circ} \text{ K} \quad B = 5 \frac{\text{Vs}}{\text{m}^2}$$

$$V_B = \left\{ \begin{array}{l} 37570 \pm 1 \\ 37750 \pm 1 \end{array} \right\} \times 10^{-6} \text{ volt}$$

$$V_o = \left\{ \begin{array}{l} 37138 \pm 1 \\ 37164 \pm 1 \end{array} \right\} \times 10^{-6} \text{ volt}$$

$$\begin{aligned} \frac{\Delta \rho}{\rho} &= .0137 \pm .000221 \\ &= .0137 \pm 1.61\% \end{aligned}$$

This is only accuracy to two significant figures.

Sample	Alloy	$\frac{R_{77^{\circ}\text{K}} - R_{4.2^{\circ}\text{K}}}{R_{273^{\circ}\text{K}} - R_{4.2^{\circ}\text{K}}}$	$\frac{R_{273^{\circ}\text{K}}}{R_{4.2^{\circ}\text{K}}}$	Deviation from Copper
A	Cu	.128	88.47	-
B		.126	89.14	-
C	Cr-Cu	.122	11.68	( 30 %)
D		.151	4.37	( 20 %)
E		.143	4.70	( 10 %)
F	Zr-Cu	.121	51.46	35 %
G		.128	55.11	25%
H		.131	43.02	35 %
J		.154	19.96	80 %

Table 1  
Zero-field Data on Samples, and  
Comparison of Magnetoresistance.

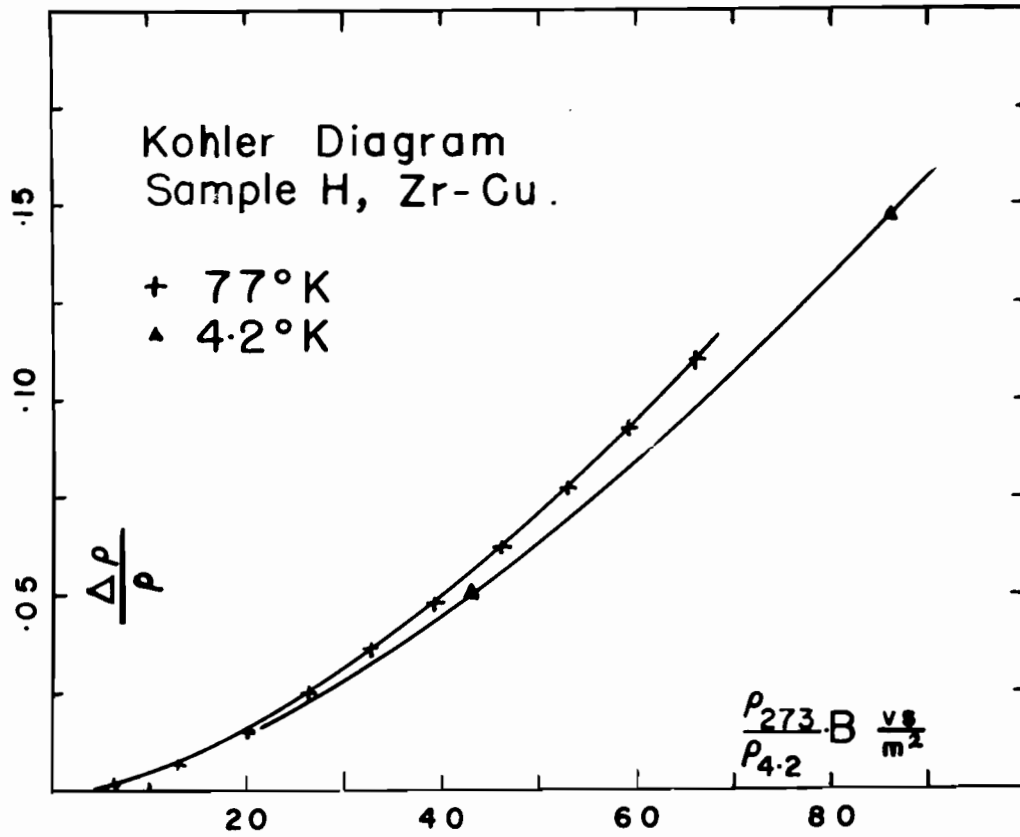


Fig. 7. Illustration of Kohler's Rule for Zirconium Copper.

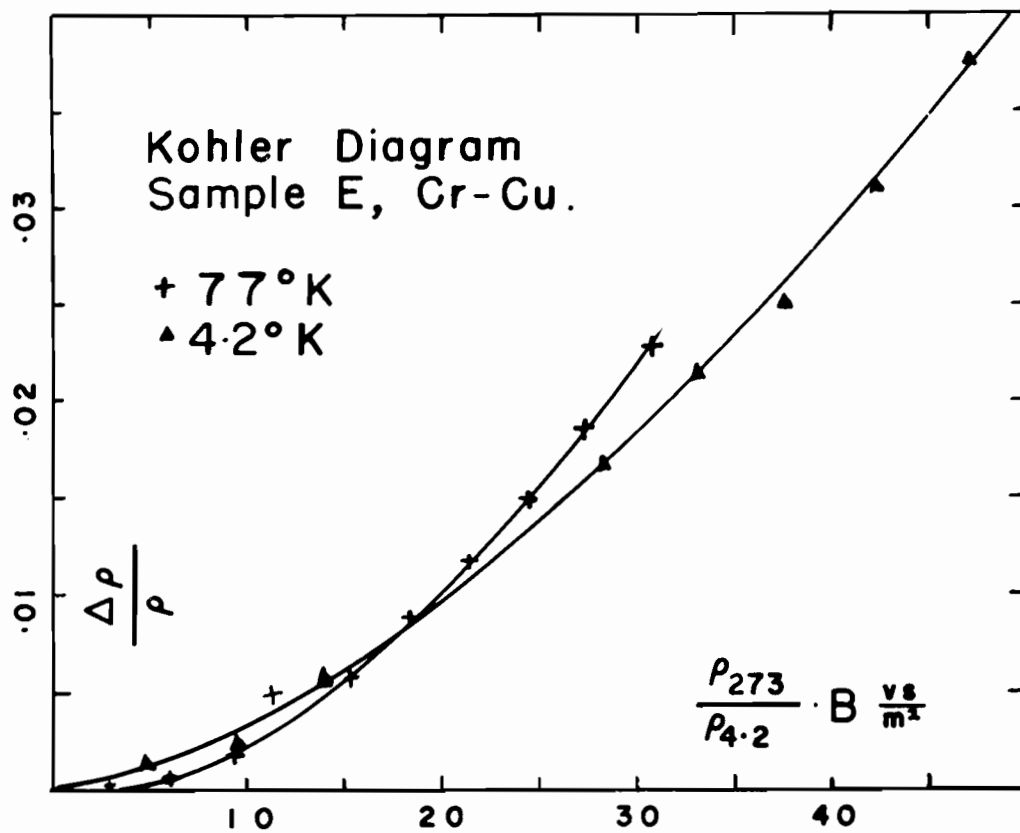


Fig. 8. Illustration of Kohler's Rule for Chromium Copper.

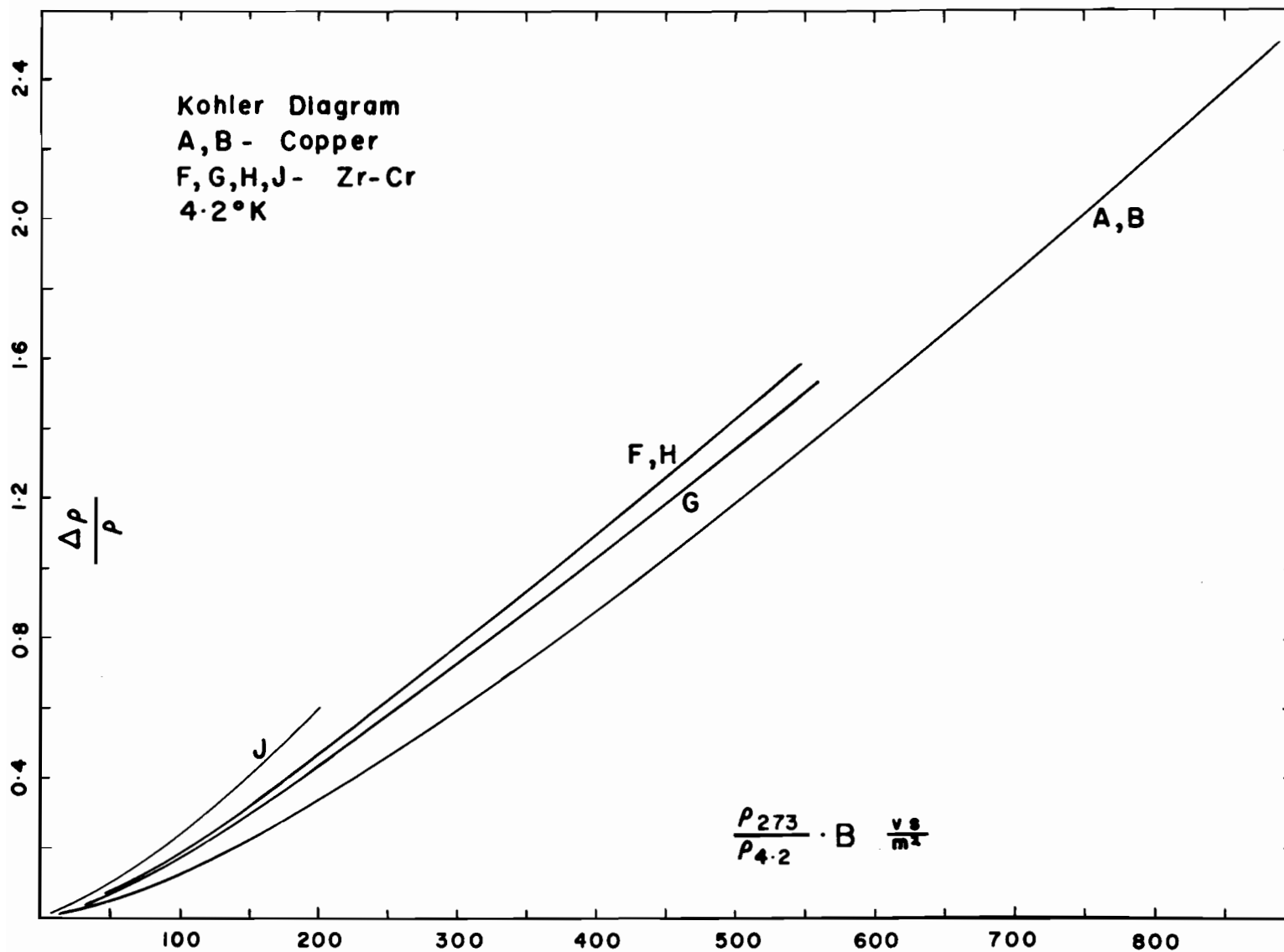


Fig. 9. Magnetoresistance of Zirconium Copper Samples.



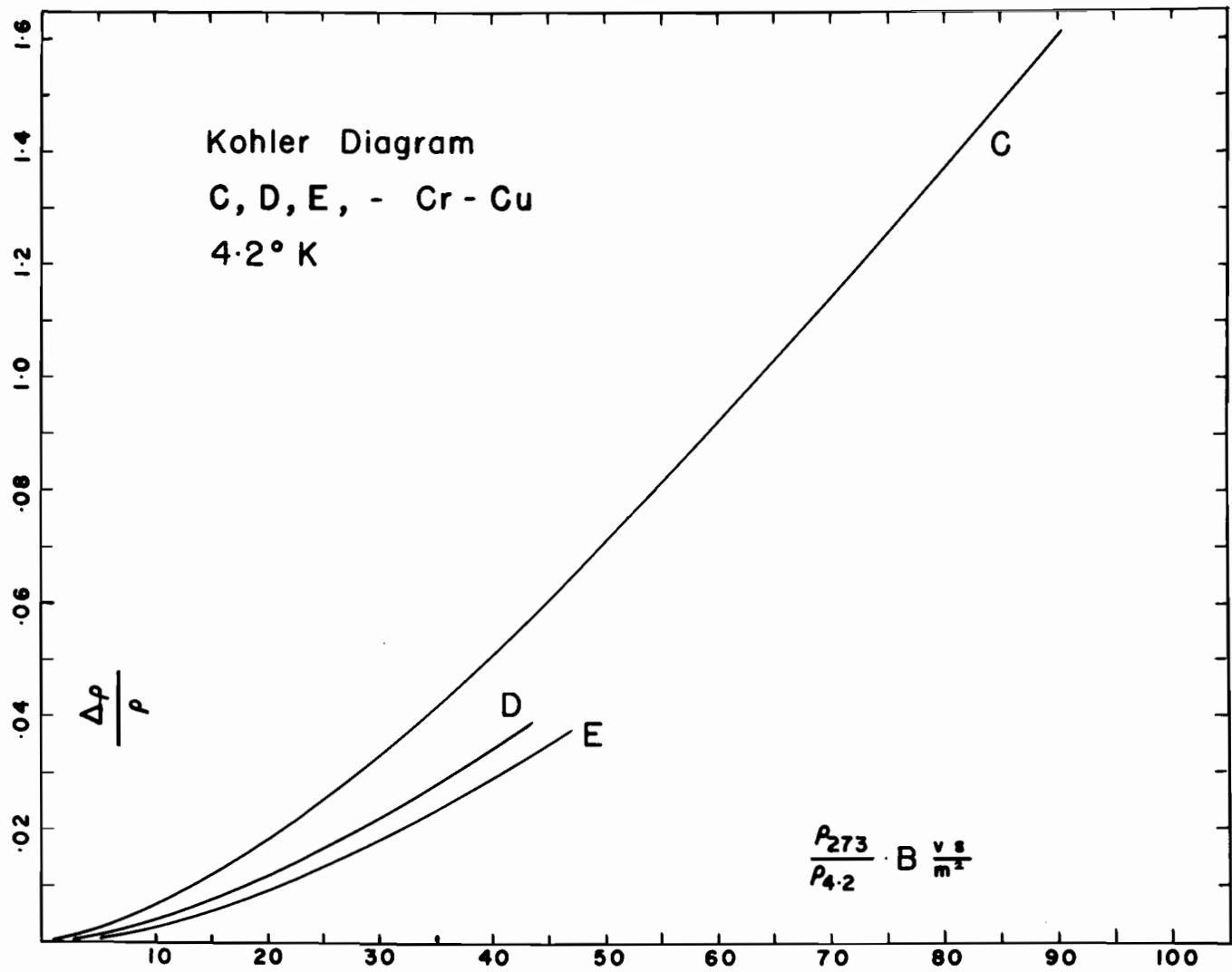


Fig. 10. Magnetoresistance of Chromium Copper Samples.

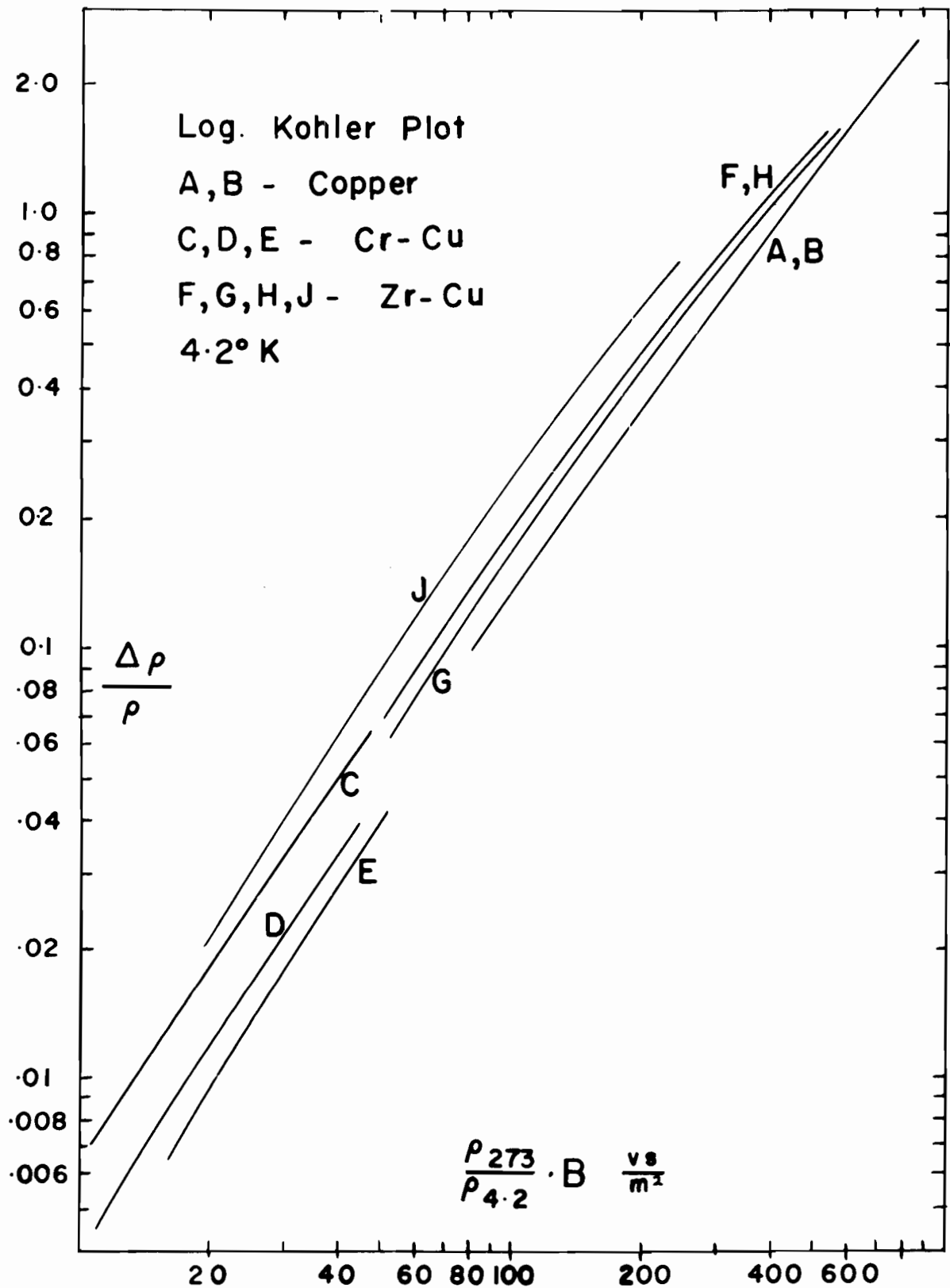


Fig. 11. Magnetoresistance of all  
 Samples at Liquid Helium Temperature.

## APPENDIX A

TRANSVERSE MAGNETORESISTANCE OF TWO BAND MODEL <sup>8</sup>

Consider a material with electrical conduction in two bands. Let the currents in the bands be  $J^{(1)}$  and  $J^{(2)}$ , and let the resistivity tensors be  $\rho^{(1)}$  and  $\rho^{(2)}$  respectively.

Both bands will see the same net electric field  $E$ , and the total current  $J$  will be

$$J_k = J_k^{(1)} + J_k^{(2)} = (\sigma_{ki}^{(1)} + \sigma_{ki}^{(2)}) E_i$$

where  $\sigma^{(1)}$  and  $\sigma^{(2)}$  are the inverse tensors of  $\rho^{(1)}$  and  $\rho^{(2)}$  respectively.

Reinverting, we have

$$E_i = \bar{\rho}_{ik} J_k$$

where  $\bar{\rho}$  is the inverse of  $(\sigma^{(1)} + \sigma^{(2)})$ . The resistivity in the direction of the current will be

$$\bar{\rho}_{ik} l_i l_k$$

where the  $l_i$  are the cosines of the total current direction.

Now the inverse of

$$\begin{pmatrix} \rho_{\perp} & \rho_H & 0 \\ \rho_H & \rho_{\perp} & 0 \\ 0 & 0 & \rho_{\parallel} \end{pmatrix} \text{ is } \begin{pmatrix} \sigma_{\perp} & \sigma_H & 0 \\ -\sigma_H & \sigma_{\perp} & 0 \\ 0 & 0 & \sigma_{\parallel} \end{pmatrix}$$

where  $\sigma_{\perp} = \frac{\rho_{\perp}}{(\rho_{\perp})^2 + (\rho_H)^2}$ ,  $\sigma_H = \frac{\rho_H}{(\rho_{\perp})^2 + (\rho_H)^2}$ ,  $\sigma_{\parallel} = \frac{1}{\rho_{\parallel}}$

Thus during inversion the field dependent term  $\rho_H$  is mixed into the diagonal terms of  $\sigma$ . It is now asserted, and can be verified by explicit calculation, that unless the bands have identical resistivity tensors,

there will be field dependent terms (containing  $\rho_H^{(1)}$  and  $\rho_H^{(2)}$ ) on the diagonal of  $\bar{\rho}$ , and the resistivity in the direction of the current will be magnetic field dependent. The basic reason for this is that each band shows no magnetoresistance only in the direction of its own current, and we are taking the resistivity in the direction of the total current.

We assume for simplicity that the second band has holes as carriers and that the Hall angle is equal and of opposite sign to the first band, and that the hole current equals the electron current. That is we assume

$$\rho_H^{(1)} = -\rho_H^{(2)} = \frac{\rho_H}{2}, \quad \rho_{||}^{(1)} = \rho_{||}^{(2)} = \frac{\rho_{||}}{2}, \quad \rho_{\perp}^{(1)} = \rho_{\perp}^{(2)} = \frac{\rho_{\perp}}{2}$$

then

$$\sigma_{\perp} = \frac{\rho_{\perp}}{(\rho_{\perp})^2 + (\rho_H)^2}, \quad \sigma_{||} = \frac{1}{\rho_{||}}, \quad \sigma_H = 0$$

$$\frac{1}{\sigma_{\perp}} = \rho_{\perp} + \frac{\rho_H^2}{\rho_{\perp}}, \quad \text{ie.} \quad \frac{\Delta \rho_{\perp}}{\rho_{\perp}} = \left( \frac{\rho_H}{\rho_{\perp}} \right)^2$$

but  $\frac{1}{\sigma_{\perp}}$

$$\frac{\rho_H}{\rho_{\perp}} = \frac{\sigma B}{n e}$$

where  $\sigma$  is the total conductivity in zero field, B is the magnetic field,

n is the carrier concentration, and e is the electronic charge.

$$\text{ie.} \quad \frac{\Delta \rho}{\rho} = \left( \frac{\sigma}{n e} \right)^2 B^2 \quad \text{from this model.}$$

APPENDIX BICE POINT RESISTIVITY OF ANNEALED SAMPLES

Annealing will change the ice point resistivity of a sample by an estimable degree. Let the initial ice point resistivity be  $\rho_0$  and initial resistance ratio  $S_0$ . Let the values after annealing be  $\rho_1$  and  $S_1$ . Assume the residual resistivity to be equal to the helium temperature resistivity and equate thermal components at the ice point.

$$\rho_0 - \rho_0/S_0 = \rho_1 - \rho_1/S_1$$

$$\text{ie } \frac{\rho_1}{\rho_0} = \frac{(S_0 - 1) S_1}{S_0 (S_1 - 1)}$$

The resulting factors vary from .75 to .87, but the initial resistivities were higher than copper. Thus since no measurements were made the assumption of equality seems justified.

REFERENCES

1. C. Kittel - Introduction to Solid State Physics (Wiley, New York, 1956)  
2nd ed.
2. L. Brillouin - Wave Propagation in Periodic Structures (McGraw Hill,  
New York, 1953) 2nd ed.
3. H. Jones - Theory of Brillouin Zones and Electronic States in Crystals  
(North Holland, Amsterdam, 1960)
4. T. Broome - Advances in Physics 3, 26 (1954)
5. H. Goldstein - Classical Mechanics (Addison Wesley, Cambridge, Mass,  
1950)
6. D.K.C. MacDonald - Handbuch der Physik 14 (Springer Verlag, Berlin,  
1956) p.137.
7. E. Gruneisen - Annalen der Physik (5) 16, 530 (1933)
8. J.-P. Jan - Solid State Physics 5, 1 (1957)
9. J.F. Nye - Physical Properties of Crystals (Clarendon Pr., Oxford, 1957)
10. J.M. Ziman - Electrons and Phonons (Clarendon Pr., Oxford, 1960)
11. Mott and Jones - Theory of the Properties of Metals and Alloys  
(Clarendon Pr., Oxford, 1936)
12. Jones and Zener - Proceedings of the Royal Society (London) A 145,  
268 (1934)
13. Lifshitz, Azbel and Kaganov - Soviet Physics J.E.T.P. 4, 41 (1957)
14. J.M. Ziman - Philosophical Magazine 3 1117 (1958)
15. P. Kapitza - Proceedings of the Royal Society (London) A-123, 292 (1929)
16. R.G. Chambers - Proceedings of the Royal Society (London) A-238,  
344 (1956)

17. S. Titeica - Annalen der Physik (5) 22, 129 (1935)
18. M. Kohler - Annalen der Physik (5) 32, 211 (1938)
19. Olsen and Rinderer - Nature 173, 682 (1954)